Mechanical anisotropy in brain tissue – experimental results and implications for modeling*

Yuan Feng[1], Ruth J. Okamoto[2], Ravi Namani[2], Guy M. Genin[2,3], Philip V. Bayly[2,4]
[1] Department of Radiation Oncology, [2] Department of Mechanical Engineering and Materials Science, [3] Department of Neurological Surgery, [4] Department of Biomedical Engineering, Washington University in St. Louis.

ABSTRACT

White matter in the brain is structurally anisotropic, consisting largely of bundles of aligned, myelin-sheathed axonal fibers. White matter is believed to be mechanically anisotropic as well. Specifically, transverse isotropy is expected locally, with the plane of isotropy normal to the local mean fiber direction. Suitable material models involve strain energy density functions that depend on the I_4 and I_5 pseudo-invariants of the Cauchy-Green strain tensor to account for the effects of relatively stiff fibers. The pseudo-invariant I_4 is the square of the stretch ratio in the fiber direction; I_5 contains contributions of shear strain in planes parallel to the fiber axis. Most, if not all, published models of white matter depend on I_4 but not on I_5. Here, we explore the small strain limits of these models in the context of experimental measurements that probe these dependencies. Models in which strain energy depends on I_4 but not I_5 can capture differences in Young's (tensile) moduli, but will not exhibit differences in shear moduli for loading parallel and normal to the mean direction of axons. We show experimentally, using a combination of shear and asymmetric indentation tests, that white matter does exhibit such differences in both tensile and shear moduli. Results highlight that: (1) hyperelastic models of transversely isotropic tissues such as white matter should include contributions of both the I_4 and I_5 strain pseudo-invariants; and (2) behavior in the small strain regime can usefully guide the choice and initial parameterization of more general material models of white matter.

INTRODUCTION

Traumatic brain injury (TBI) is a common cause of death and disability in the United States (Coronado, 2011). In such injuries, linear and angular acceleration of the head leads to shearing and stretching of brain parenchyma (Bayly, 2005, Margulies, 1992, Clayton, 2012, Gennarelli, 1982). Prediction of these injuries remains elusive, though it is a subject of intense research. Computer simulation methods, predominantly finite element (FE) simulations, have been proposed for prediction of injuries and development of preventive strategies (Ueno, 1995, Zhang, 2004). Predicted strains from simulations can be correlated with injury markers (McAllister, 2012) using strain-based thresholds for cellular and tissue injury determined in vitro (Wright, 2012, LaPlaca, 2005, Morrison, 2003).

* Major results included here have been accepted for publication in the Journal of the Mechanical Behavior of Biomedical Materials.

White matter tissue appears to be preferentially injured during brain trauma (Smith, 2000), and the mechanics of white matter are important for predicting its deformation and associated injury. Since white matter consists predominantly of aligned axonal fibers and their myelin sheaths, it is hypothesized to be mechanically anisotropic, in contrast to gray matter, which is structurally isotropic (Prange, 2000). More specifically, where fibers are well-aligned, white matter is expected to be transversely isotropic with the fiber axis normal to the plane of isotropy.

The literature largely supports this hypothesis, though estimates of specific parameter vary. (Nicolle, 2005, Velardi, 2006, Romano, 2012, Miller, 2002, Arbogast, 1998, Ning, 2006, Prange, 2002). Transversely isotropic materials may, in general, exhibit anisotropy in both shear and tension with respect to the fiber axis (Spencer, 1984). To our knowledge, prior experimental studies of white matter (Hrapko, 2008, Prange, 2002, Velardi, 2006) have focused on either shear or tensile anisotropy, but not both. Measurement of anisotropy in both shear and classical tensile tests requires separate samples, as gripping brain tissue for tensile tests damages the tissue. To overcome this measurement problem, dynamic shear tests can be combined with subsequent asymmetric indentation tests on the same sample, to measure the anisotropy of brain tissue. This protocol involves both fiber-matrix shear and fiber stretch (Namani, 2012). Each test requires only simple fixtures to hold the sample, and is non-destructive at small strains. Subject to certain assumptions described below, the combination can be used to estimate all the parameters of an incompressible, transversely isotropic, linear elastic model of brain tissue.

The goal of our study is to clarify what features of constitutive models are needed to capture the mechanical anisotropy (mainly transversely isotropy) of white matter. The predicted response of transversely isotropic material in the infinitesimal strain limit is compared to relatively simple experiments that identify the specific contributions of fiber stretch and fiber-matrix interaction. We tested samples of white matter (corpus callosum) and gray matter (cortex) from lamb brains, using a combination of dynamic shear testing (DST) (Okamoto, 2011) and asymmetric indentation tests (Namani, 2012). White matter was found to be anisotropic in both shear and indentation, while gray matter exhibited isotropic behavior. These results, while obtained in the small-strain regime, imply that in an accurate hyperelastic model of white matter, the strain energy function should depend on both I_4 and I_5.

.

METHODS

General hyperelasticity

White matter is fibrous tissue in which a clearly-defined, dominant fiber direction is typical. For example, fibers are predominantly oriented left-to-right in the corpus callosum, which connects the brain's hemispheres. We define the fiber direction to be the $\mathbf{x}_1$ direction in Cartesian coordinates, so the plane of isotropy is perpendicular to $\mathbf{x}_1$ (Fig. 1). If $\mathbf{F}=\partial\mathbf{x}/\partial\mathbf{X}$ is the deformation gradient, where $\mathbf{X}$ is a material vector in the reference configuration and $\mathbf{x}$ is the corresponding spatial vector in the deformed configuration, the right and left Cauchy-Green tensors are $\mathbf{C}=\mathbf{F}^T\mathbf{F}$ and $\mathbf{b}=\mathbf{F}\mathbf{F}^T$. The volume ratio between the deformed and undeformed configurations is given by $J = \det\mathbf{F}$. The corresponding principal invariants of $\mathbf{C}$ and $\mathbf{b}$ are (Holzapfel, 2000, Spencer, 1984) I_1 to I_5 and the strain energy function ψ can be written generally in terms of the invariants:

$$\psi = \psi\left(I_1, I_2, I_3, I_4, I_5\right). \tag{1}$$

The general form of the Cauchy stress in terms of the invariants defined above, writing $\psi_i = \partial\psi/\partial I_i$ (i=1, ..., 5), is:

$$\boldsymbol{\sigma} = 2I_3^{-1/2}\left[\psi_1\,\mathbf{b} + \psi_2\left(I_1\,\mathbf{b} - \mathbf{b}^2\right) + I_3\,\psi_3\,\mathbf{I} + \psi_4\,\mathbf{a}\otimes\mathbf{a} + \psi_5\left(\mathbf{a}\otimes\mathbf{b}\,\mathbf{a} + \mathbf{a}\,\mathbf{b}\otimes\mathbf{a}\right)\right]. \tag{2}$$

Requiring both strain energy density and Cauchy stress to vanish in the undeformed (reference) state, leads to the following constraints on the strain energy function:

$$\psi\left(3,3,1,1,1\right) = 0 \tag{3}$$

$$\left(\psi_1 + 2\psi_2 + I_3\,\psi_3\right)_{(3,3,1,1,1)} = 0\text{, and} \tag{4}$$

$$\left(\psi_4 + 2\psi_5\right)_{(3,3,1,1,1)} = 0 \tag{5}$$

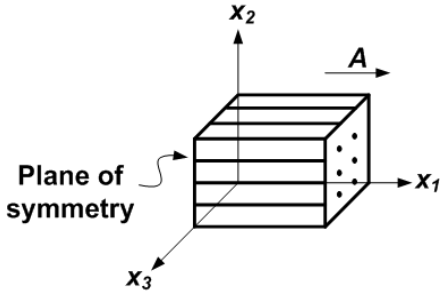

Figure 1**.** Basic model of a transversely isotropic (fibrous) material. Vector **A** indicates the fiber direction in the reference configuration. The plane of isotropy is perpendicular to x_1.

Transversely isotropic linear elastic models

The incremental behavior of a hyperelastic material can be described using the equations of linear elasticity (Holzapfel, 2000). The elasticity matrix of a linearly elastic transversely isotropic material with $\mathbf{X}_1$ as its axis of symmetry has five independent parameters and can be written as (Bower, 2010):

$$\begin{bmatrix}\sigma_{11}\\ \sigma_{22}\\ \sigma_{33}\\ \sigma_{23}\\ \sigma_{13}\\ \sigma_{12}\end{bmatrix} = [c_{ij}]\begin{bmatrix}\varepsilon_{11}\\ \varepsilon_{22}\\ \varepsilon_{33}\\ 2\varepsilon_{23}\\ 2\varepsilon_{13}\\ 2\varepsilon_{12}\end{bmatrix} = \begin{bmatrix} c_{11} & c_{12} & c_{12} & & & \\ & c_{22} & c_{23} & & 0 & \\ & & c_{22} & & & \\ & & & \dfrac{c_{22}-c_{23}}{2} & & \\ & SYM & & & c_{55} & \\ & & & & & c_{55}\end{bmatrix}\cdot\begin{bmatrix}\varepsilon_{11}\\ \varepsilon_{22}\\ \varepsilon_{33}\\ 2\varepsilon_{23}\\ 2\varepsilon_{13}\\ 2\varepsilon_{12}\end{bmatrix} \tag{6}$$

Define $\psi_i = \partial\psi/\partial I_i$ and $\psi_{ij} = \partial^2\psi/\partial I_i\partial I_j$ (i,j = 1,...,5), we can show (Merodio, 2003) that the elasticity matrix can thus be written as:

$$[c_{ij}] = \begin{bmatrix} c_{11} & c_{12} & c_{12} & & & & \\ c_{12} & c_{22} & c_{23} & & & & \\ c_{12} & c_{23} & c_{22} & & & & \\ & & & \psi_1+\psi_2 & & & \\ & & & & \psi_1+\psi_2+2\psi_5 & & \\ & & & & & \psi_1+\psi_2+2\psi_5 & \end{bmatrix} \tag{7}$$

where the 1-direction is aligned with **A**, and subscripts on ψ again represent partial differentiation with respect to the five invariants. Both I_4 and I_5 terms contribute to the difference between the elastic moduli in the principal directions:

$$c_{11} - c_{22} = 4\psi_{44} + 16\psi_{45} + 16\psi_{45} + 8\psi_5 + 2(c_{12} - c_{23}) \tag{8}$$

We also observe that:

$$c_{55} - c_{44} = 2\psi_5 \tag{9}$$

which shows that ψ must depend on I_5 if the material exhibits different shear moduli in different orthogonal planes parallel and normal to the fiber axis for small strain. Since ψ_5 is evaluated in the reference configuation, the form of ψ should be chosen so that $(\psi_5)_{(3,3,1,1,1)}$ is not zero. Eqs. (8) and (9) are general results that illustrate the implications of small-strain behavior for general hyperelastic models.

Prior studies, as well as our own experiments, suggest that white matter is nearly-incompressible and anisotropic in both uniaxial stretch and simple shear deformations; i.e. in both cases the stress-strain relationships depend on whether displacements are imposed parallel or perpendicular to the fiber axis. To analyze this behavior, we find that models written in terms of an isochoric pseudo-invariant $\bar{I}_5^*$ that contains no contribution from fiber stretch adopt particularly convenient forms. The deformation gradient may be decomposed into dilatational and distortional parts (Holzapfel, 2000): $\mathbf{F} = J^{1/3}\overline{\mathbf{F}}$. The modified right, left Cauchy-Green tensors, and fiber direction vector are:

$$\overline{\mathbf{C}} = \overline{\mathbf{F}}^T\overline{\mathbf{F}} = J^{-2/3}\mathbf{C},\ \overline{\mathbf{b}} = \overline{\mathbf{F}}\overline{\mathbf{F}}^T = J^{-2/3}\mathbf{b}, \text{ and } \overline{\mathbf{a}} = J^{-1/3}\mathbf{a} \tag{10}$$

where **C** and **b** are the right and left Cauchy-Green tensors defined earlier. The corresponding modified principal invariants are:

$$\bar{I}_1 = J^{-2/3}I_1,\ \bar{I}_2 = J^{-4/3}I_2,\ J = I_3^{1/2},\ \ \bar{I}_4 = J^{-2/3}I_4, \text{ and } \bar{I}_5 = J^{-4/3}I_5 \tag{11}$$

To describe the anisotropic component of the strain energy function in a simple material model, we combine a quadratic term of $\bar{I}_4$ that describes the additional strain energy due to fiber stretch, and a term proportional to $\bar{I}_5^* = \bar{I}_5 - \bar{I}_4^2$ that describes the effect of fiber-matrix interactions. The isochoric component of strain energy for this model is:

$$\Psi_{isochoric} = \frac{\mu}{2}\left[(\bar{I}_1 - 3) + \zeta(\bar{I}_4 - 1)^2 + \phi\bar{I}_5^*\right]. \tag{12}$$

Here μ is the isotropic shear modulus, and ζ and ϕ are parameters of the anisotropic model. Finally, we express the volumetric component of strain energy in terms of a bulk modulus κ and the change in volume (Ning, 2006, Bower, 2010):

$$\Psi_{volumetric} = \frac{\kappa}{2}\left(J-1\right)^2 \tag{13}$$

To describe nearly-incompressible materials like brain tissue, κ κwill have a large value relative to the quantities μ, $\mu\zeta$ and $\mu\phi$. The complete candidate strain energy function is thus:

$$\frac{\mu}{2}\left[\left(\bar{I}_1-3\right)+\ \zeta\left(\bar{I}_4-1\right)^2+\phi\ \bar{I}_5^*\ \right]+\frac{\kappa}{2}\left(J-1\right)^2 \tag{14}$$

and the corresponding Cauchy stress tensor is:

$$\begin{aligned}\boldsymbol{\sigma}=&\mu J^{-1}\bar{\mathbf{b}}\ +\left[\kappa\left(J-1\right)-2\mu J^{-1}\left(\frac{1}{6}\bar{I}_1+\frac{\zeta\bar{I}_4}{3}\left(\bar{I}_4-1\right)+\frac{\phi}{3}\bar{I}_5^*\right)\right]\mathbf{I}+\\&2\mu J^{-1}\left(\zeta\left(\bar{I}_4-1\right)-\phi\bar{I}_4\ \right)\bar{\mathbf{a}}\otimes\ \bar{\mathbf{a}}+\ \mu\phi\ J^{-1}\ \left(\bar{\mathbf{a}}\otimes\ \bar{\mathbf{b}}\,\bar{\mathbf{a}}+\bar{\mathbf{a}}\,\bar{\mathbf{b}}\otimes\bar{\mathbf{a}}\right)\end{aligned} \tag{15}$$

As required, the values of Ψ and of all components of $\boldsymbol{\sigma}$ equal zero in the reference configuration (Eqs.(3)-(5)).

Sample preparation

The material model parameters can be estimated from a combination of (1) simple shear with displacement either parallel or perpendicular to the fiber axis and (2) indentation with a tip of rectangular cross-section, in which the long axis of the tip is aligned either parallel or perpendicular to the fiber axis, with both tests performed on the same sample (Namani, 2012)

Lamb heads (8 to 10 months of age) were obtained from a local slaughterhouse one to two hours post-mortem. The top of the skull was resected by cutting the bone on four sides. The dura mater, arachnoid and pia matter were resected with fine scissors, and the two hemispheres were separated. Gray matter tissue samples were harvested from the temporal lobe (Fig. 2 (a,c)) close to the cerebellum. The cerebellum was separated from the two lobes by cutting the tentorium, and white matter tissue samples were harvested from the corpus callosum (Fig. 2 (b,c,)), where axonal fibers can be seen running across and connecting the left and the right brain hemispheres. Tissue samples were sliced using a vibrating microtome (Vibratome®, series 1000, St. Louis, MO), and test samples were punched from the cross-section to obtain predominantly gray matter (Fig. 2 (d)) or white matter (Fig. 2 (e)). Circular punched samples were ~2.8 mm thick and ~15.6 mm in diameter. All samples were submerged in ice-cold artificial cerebrospinal fluid (CSF) (Alexander, 2005) before testing, which was conducted within five hours post-mortem as recommended by Garo et al. (2007). Testing was performed at room temperature (21°C- 23°C).

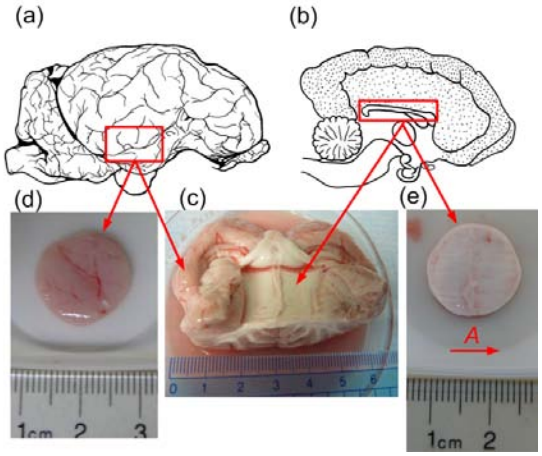

Figure 2**.** (a) Lateral sagittal view of lamb brain. The red box indicates the temporal lobe region from which gray matter samples were harvested. (b) Medial sagittal view of the lamb brain; the red box indicates the corpus callosum region from which white matter samples were harvested. (c) Portion of lamb brain showing the corresponding region where (d) gray matter sample and (e) white matter sample were dissected and punched for experiment. The ruler below the sample has 1mm scale increments. Vector A indicates the axonal fiber direction in the white matter sample.

Dynamic shear testing (DST) and asymmetric indentation

The complex shear modulus was measured using a dynamic shear testing (DST) device (Namani, 2012, Okamoto, 2011). Samples were held between two parallel plates with rough (sandpaper) surfaces and compressed 5% to ensure consistent contact and normal force. Vibratory shear displacement u_x of the lower plate was produced by a voice coil, while shear force, F_s, was measured on the stationary upper plate. Data were acquired with a SigLab 20-22 data acquisition system (Spectral Dynamics, Inc., San Jose, CA) and stored on a PC. White matter samples were tested with the fiber direction either parallel (test 1, Fig. 3a) or perpendicular (test 2, Fig. 3b) to the direction of oscillation. Gray matter samples were also tested in two orientations, rotating the sample by 90° after the first test, with the first test marked as test A and second test as test B. The average shear stress on the sample's stationary surface is given by $\tau = F_s / A_s$, where A_s is the area of the sample's circular face. The nominal shear strain was estimated as $\gamma = u_x / h = \left(U_x \cos(\omega t)\right) / h$, where U_x (~0.03 mm) is the amplitude of the horizontal shear oscillation, h is the sample thickness, and $\omega = 2\pi f$, where f is the frequency (20 to 200 Hz). The complex shear modulus, μ^*, was calculated from τ and γ:

$$\mu^*(\omega) = \frac{\tau(i\omega)}{\gamma(i\omega)} = \frac{F_s(i\omega)/A_c}{u_x(i\omega)/h} = \mu'(\omega) + i\mu''(\omega) \tag{14}$$

where μ' is the storage modulus and μ'' is the loss modulus.

The indentation stiffness of each tissue sample was measured after the DST test. We used a custom-built asymmetric indentation device and adopted a 3-step indentation protocol used previously (Namani, 2012). The rectangular stainless steel indenter head was 19.1 mm long × 1.6 mm wide. As with DST, we tested each sample in two configurations, rotated by 90°. White matter samples were tested with axonal fiber tracts parallel (∥, Fig. 3c) or perpendicular (⊥, Fig. 3d) to the longer side of the rectangular indenter head. Gray matter samples were placed on the device in an arbitrary orientation and then rotated by 90° after the first test, with the first and

second test results noted as A and B, respectively. Each sample was indented to a depth of 5% of its thickness and then held in that position for 1 minute for tissue relaxation, which is sufficient for brain tissue to fully relax to a steady state isometric force (Gefen, 2004, van Dommelen, 2010, Elkin, 2011, Prevost, 2011). This process was repeated for a total of three indentation steps, reaching approximately 5%, 10%, and 15% of the sample thickness, respectively. Each indentation step was completed within 0.5 sec with an average strain rate during indentation of 0.1 s^{-1}. The indenter was actuated by a piezo-electric actuator (Model M-227.5, Physik Instrumente, Auburn, MA) and the indentation force, F_i, was measured by a load cell (Honeywell Sensotec, Model 31, 150 g), where indices i = 1, 2, 3 represent the three indentation steps. The vertical displacement of the indenter, d_i, was measured by a non-contact proximity probe (Model 10001-5MM, Metrix Instrument, Houston, TX). Custom written Matlab programs (The Mathworks, Natick, MA) were used for data acquisition and system control. The force-displacement curve during indentation was analyzed and the portion with approximately constant indentation velocity was fit to a line with a slope corresponding to the indentation stiffness $k = F_i / d_i$.

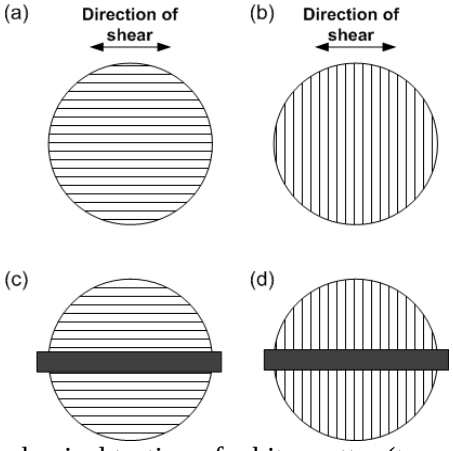

Figure 3 Sample configurations for mechanical testing of white matter (top view). In shear tests, each white matter sample was tested with axonal fibers (a) parallel and (b) perpendicular to the direction of imposed displacement. In indentation tests, each white matter sample was tested with axonal fibers (a) parallel and (b) perpendicular to the long side of the indenter head.

RESULTS

A total of 12 white matter samples and 9 gray matter samples were tested. For 6 of 12 white matter samples $k_{\perp}$ was measured before $k_{\parallel}$, and for the remaining six, $k_{\parallel}$ was measured before $k_{\perp}$. Typical DST measurements for both gray and white samples are shown in Fig. 4(a-b). The peak horizontal displacement of the flexure, U_x, was 0.03 mm, corresponding to a nominal shear strain of ~1%. Typical indentation measurements for both gray and white matter samples are shown in Fig. 4(c-d). Consistent mechanical anisotropy was observed in both DST and indentation tests in corpus callosum white matter tissue.

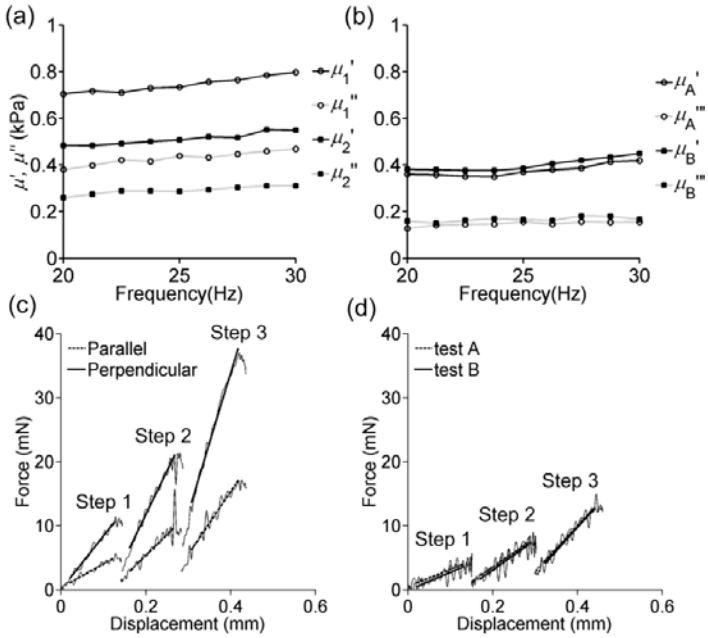

Figure 4 Representative DST and indentation data. (a) DST of a white matter sample tested with the shear loading applied in a plane parallel to the axonal fiber direction (μ_1), or in a plane perpendicular to the axonal fiber direction (μ_2). (b) Gray matter sample tested in one orientation (μ_A) and then rotated by 90° (μ_B). Storage and loss modulus components of the complex modulus, $\mu' + i\,\mu''$, were measured using DST over the frequency range 20-200 Hz (only 20-30 Hz is shown). Force-displacement curves in 3-step indentation were recorded for (c) white matter samples tested with the fiber direction either parallel (||) or perpendicular (⊥) to the long side of the indenter head, and (d) gray matter samples tested in one orientation (test A) and rotated by 90° (test B). The solid lines are linear fits to data obtained when the indentation head is at a constant velocity.

Results of shear tests: White matter samples were stiffer when tested with the fibers parallel to the direction of shear (Fig. 3a), while no orientation dependence was detected for the shear moduli of gray matter samples. To compare shear moduli between samples, we averaged the storage and loss moduli of each sample at frequencies between 20 and 30 Hz. We calculated the estimated shear wavelengths based on the average shear moduli values and found that the wavelengths were at least 6 times longer than the thickness of the sample, meaning that inertial effects could be neglected relative to elastic and viscoelastic effects.

The average storage and loss moduli for white and gray matter samples from the DST tests are shown in Fig. 5a. The storage and loss moduli for white matter were significantly larger when the samples were tested with the primary axonal fiber direction parallel to the direction of shear regardless of the order in which the two orientations were tested. However, no significant differences were observed for gray matter between the two orientations tested (Fig. 5b). The storage and loss moduli ratios (μ_1'/μ_2' and μ_1''/μ_2'') of white matter samples were 1.41 ± 0.26 and 1.43 ± 0.29 respectively; for gray matter samples, the storage and loss modulus ratio (μ_A'/μ_B' and μ_A''/μ_B'') were 0.96 ± 0.11 and 0.96 ± 0.15 respectively.

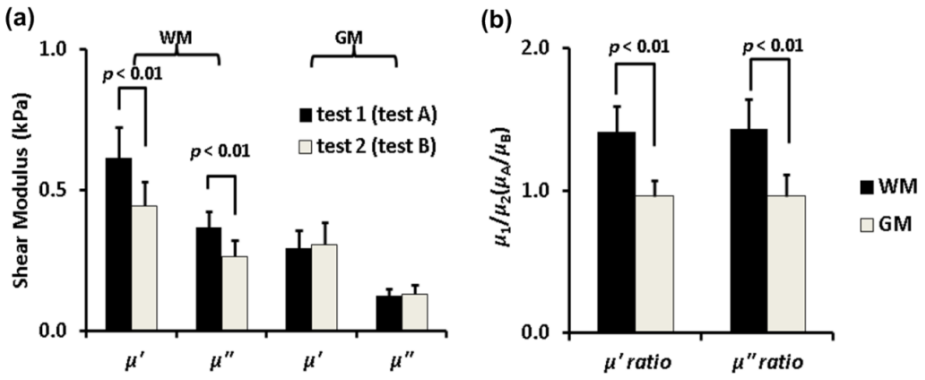

Figure 5 (a) Comparison of storage and loss components of the complex shear modulus of white matter (n = 12 samples) and gray matter (n = 9 samples). (b) Ratios of complex modulus components of white matter and gray matter, estimated by DST over frequency range of 20-30 Hz. Differences between storage moduli (μ_1' and μ_2') and between loss moduli (μ_1'' and μ_2'') for white matter samples were statistically significant (student's t-test, $p < 0.01$). Differences between storage moduli ratios (μ_1'/μ_2' and μ_A'/μ_B') and between loss moduli ratios (μ_1''/μ_2'' and μ_A''/μ_B'') for white and gray matter samples were statistically significant (student's t-test, p<0.01).

Results of indentation tests: White matter samples appeared stiffer when indented with fibers perpendicular to the long side of the indenter head (Fig. 3d) compared to indentation when fibers were parallel to the long axis. In contrast, gray matter samples exhibited similar indentation stiffness in both the first and second tests. The indentation stiffness values for all samples are summarized in Fig. 6a; indentation stiffness ratios ($k_\perp/k_\parallel$ or k_A/k_B) are compared for gray and white matter in Fig. 6b. Average values are also given in Table 1. For white matter samples, $k_\perp$ was significantly greater than $k_\parallel$, regardless of the order in which the two tests were performed. This was true for each indentation step, although the stiffness ratio $k_\perp/k_\parallel$ decreased for the second and third indentation step (2.3 ± 0.7 and 2.1 ± 0.6 respectively). For gray matter samples, there was no signicant difference between k_A and k_B and the stiffness ratio k_A/k_B was not significantly different than one for any of the three steps. The relatively large standard deviations in the stiffness ratios was likely due to the uncertainty in establishing contact and local variations in thickness of individual samples. In addition, $k_\parallel$ of white matter samples for each indentation step was not significantly greater than k_A or k_B of gray matter samples for the corresponding step (Fig. 6).

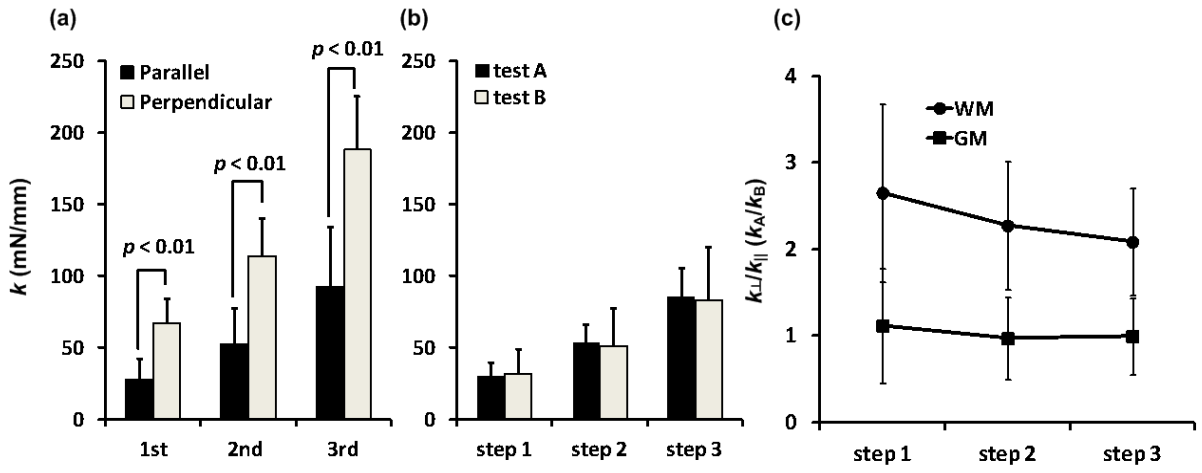

Figure 6 (a) Comparison of indentation stiffness of (a) white matter (n = 12 samples) and (b) gray matter (n = 9 samples) for each indentation step. Indentation stiffness measured for white matter is denoted $k_{\parallel}$ (for axonal fiber direction parallel to the long axis of the rectangular indenter head) and $k_{\perp}$ (fiber axis perpendicular to the long axis of indenter). Indentation stiffness measured for gray matter is denoteed k_A and k_B for two orientations of the sample 90° apart. At each indentation step, the difference between $k_{\parallel}$ and $k_{\perp}$ was significant (student's t-test, $p < 0.01$), but the difference between k_A and k_B was not significant (c) Indentation stiffness ratio of gray and white matter. Differences in the indentation ratio ($k_{\perp}/k_{\parallel}$ or k_A/k_B) for each indentation step between white matter (WM) and gray matter (GM) samples were significantly different (student's t-test $p < 0.01$).

DISCUSSION

In this study, we investigated the requirements for general hyperelastic, transversely isotropic models of white matter in the brain. Clear mechanical anisotropy of white matter was observed in both shear and indentation tests, while gray matter tissue appeared consistently isotropic. We observe that, because white matter exhibits anisotropy in small deformations involving shear without fiber stretch, as well as during deformations involving fiber stretch, any strain energy function describing it must depend on *both* of the two pseudo-invariants I_4 and I_5.

The shear storage moduli measured in our study at 20-30 Hz ranged approximately from 0.40 -0.62 kPa for white matter and 0.30 kPa for gray matter. These values are within the broad range of values reported in prior research on mammalian brain tissue (Chatelin, 2010) and consistent with previous tests of white matter tissue (corona radiata) under oscillatory shear tests at 23°C (Hrapko, 2008).

Our findings that white matter from the corpus callosum is mechanically anisotropic and gray matter is mechanically isotropic are consistent with most prior studies. Our observation that the sample is stiffer when shear is applied in the plane parallel to the fibers, compared to shear in the plane perpendicular to the fibers, is consistent with the observations of Prange and Margulies (2002) for the corona radiata, though it differs from their findings in the corpus callosum. Hrapko and co-authors (2008) also found that white matter tissue from the corona radiata region was mechanically anisotropic, with a stiffness ratio between maximum and minimum directions

of about 1.3. We note also some conflicting evidence; early studies using human brain tissue (Shuck, 1972) suggest that white matter tissue from the corona radiata is isotropic in shear. A more recent study using DST and rotational rheometry (Nicolle, 2005) also concluded that porcine white matter tissue from the corona radiata does not exhibit significant anisotropy in shear.

In the majority of hyperelastic, transversely isotropic models of fibrous tissue in the literature, the strain energy function is assumed to depend on the pseudo-invariant I_4 but not on I_5 (Ning, 2006, Velardi, 2006, Qiu, 1997). Such material models will predict the same shear modulus for simple shear in planes parallel to the fiber axis as for shear in planes perpendicular to the fiber axis (Qiu, 1997). This is inconsistent with the anisotropy that we observed in our experimental shear tests: the shear modulus is larger when displacement is applied along the fiber axis. We show that a simple hyperelastic model can explain the observed mechanical response of white matter, as long as it includes contributions from both I_4 and I_5 in the strain energy density function.

In this study we also demonstrate the utility and limitations of combining two types of tests to probe mechanical anisotropy of brain tissue. These tests were selected because they are both sensitive to the degree of mechanical anisotropy under distinct types of mechanical loading. A more direct measurement of the contribution of I_4 might be obtained with tensile tests of brain tissue samples (Velardi, 2006); however, these tests are challenging, due to difficulty in gripping the samples and minimizing edge (or end) effects in small samples.

CONCLUSIONS

The combination of shear and indentation tests shows that gray matter is approximately mechanically isotropic, while white matter appears to be mechanically anisotropic (transversely isotropic) in both extension and shear with respect to the dominant axonal fiber direction. This anisotropy is likely due to both fiber stretch and fiber-matrix interactions. To account for this behavior, any hyperelastic material model of white matter should include contributions of both I_4 and I_5 in its strain energy density function.

ACKNOWLEDGEMENTS

Funding was provided by NIH grant NS055951. The authors would like to thank Gang Xu for providing technical help on using vibratome and Long Huang for making the lamb brain anatomy illustration.

REFERENCES

Alexander, G M, and D W Godwin. "Presynaptic Inhibition of Corticothalamic Feedback by Metabotropic Glutamate Receptors." *J Neurophysiol* 94 (2005): 163-75.

Arbogast, K. B., and S. S. Margulies. "Material Characterization of the Brainstem from Oscillatory Shear Tests." *J Biomech* 31, no. 9 (Sep 1998): 801-7.

Bayly, P V, T S Cohen, E P Leister, D Ajo, E C Leuthardt, and G M Genin. "Deformation of the Human Brain Induced by Mild Acceleration." *J Neurotrauma* 22 (2005): 845-56.

Bower, Allan F. *Applied Mechanics of Solids*. 1st ed. Boca Raton, FL: CRC Press, 2010.

Chatelin, S, A Constantinesco, and R Willinger. "Fifty Years of Brain Tissue Mechanical Testing: From in Vitro to in Vivo Investigations." *Biorheology* 47 (2010): 255-76.

Clayton, E. H., G. M. Genin, and P. V. Bayly. "Transmission, Attenuation and Reflection of Shear Waves in the Human Brain." *J R Soc Interface* (Jun 12 2012).

Coronado, V. G., L. Xu, S. V. Basavaraju, L. C. McGuire, M. M. Wald, M. D. Faul, B. R. Guzman, and J. D. Hemphill. "Surveillance for Traumatic Brain Injury-Related Deaths--United States, 1997-2007." *MMWR Surveill Summ* 60, no. 5 (May 6 2011): 1-32.

Elkin, B. S., A. Ilankova, and B. Morrison, 3rd. "Dynamic, Regional Mechanical Properties of the Porcine Brain: Indentation in the Coronal Plane." *J Biomech Eng* 133, no. 7 (Jul 2011): 071009.

Garo, A., M. Hrapko, J. A. van Dommelen, and G. W. Peters. "Towards a Reliable Characterisation of the Mechanical Behaviour of Brain Tissue: The Effects of Post-Mortem Time and Sample Preparation." *Biorheology* 44, no. 1 (2007): 51-8.

Gefen, A, and S S Margulies. "Are in Vivo and in Situ Brain Tissues Mechanically Similar?". *J Biomech* 37 (2004): 1339-52.

Gennarelli, T. A., L. E. Thibault, J. H. Adams, D. I. Graham, C. J. Thompson, and R. P. Marcincin. "Diffuse Axonal Injury and Traumatic Coma in the Primate." *Ann Neurol* 12, no. 6 (Dec 1982): 564-74.

Holzapfel, Gerhard. *Nonlinear Solid Mechanics: A Continuum Approach for Engineering*. John Wiley & Sons, Inc., 2000.

Hrapko, M., J. A. van Dommelen, G. W. Peters, and J. S. Wismans. "Characterisation of the Mechanical Behaviour of Brain Tissue in Compression and Shear." *Biorheology* 45, no. 6 (2008): 663-76.

LaPlaca, M. C., D. K. Cullen, J. J. McLoughlin, and R. S. Cargill, 2nd. "High Rate Shear Strain of Three-Dimensional Neural Cell Cultures: A New in Vitro Traumatic Brain Injury Model." *J Biomech* 38, no. 5 (May 2005): 1093-105.

Margulies, Susan S, and lawrence e. Thibault. "A Proposed Tolerance Criterion for Diffuse Axonal Injury in Man." *J Biomech* 25 (1992): 917-23.

McAllister, Thomas W, James C Ford, Songbai Ji, Jonathan G Beckwith, Laura A Flashman, Keith Paulsen, and Richard M Greenwald. "Maximum Principal Strain and Strain Rate Associated with Concussion Diagnosis Correlates with Changes in Corpus Callosum White Matter Indices." *Ann Biomed Eng* 40 (2012): 127-40.

Merodio, J., and R.W. Ogden. "Instabilities and Loss of Ellipticity in Fiber-Reinforced Compressible Non-Linearly Elastic Solids under Plane Deformation." *International Journal of Solids and Structures* 40 (2003): 4707-27.

Miller, K., and K. Chinzei. "Mechanical Properties of Brain Tissue in Tension." *Journal of Biomechanics* 35, no. 4 (Apr 2002): 483-90.

Morrison, B., 3rd, H. L. Cater, C. C. Wang, F. C. Thomas, C. T. Hung, G. A. Ateshian, and L. E. Sundstrom. "A Tissue Level Tolerance Criterion for Living Brain Developed with an in Vitro Model of Traumatic Mechanical Loading." *Stapp Car Crash J* 47 (Oct 2003): 93-105.

Namani, R., Y. Feng, R. J. Okamoto, N. Jesuraj, S. E. Sakiyama-Elbert, G. M. Genin, and P. V. Bayly. "Elastic Characterization of Transversely Isotropic Soft Materials by Dynamic Shear and Asymmetric Indentation." *J Biomech Eng* 134, no. 6 (Jun 2012): 061004.

Nicolle, S, M Lounis, R Willinger, and J F Palierne. "Shear Linear Behavior of Brain Tissue over a Large Frequency Range." *Biorheology* 42 (2005): 209-23.

Ning, X, Q Zhu, Y Lanir, and S S Margulies. "A Transversely Isotropic Viscoelastic Constitutive Equation for Brainstem Undergoing Finite Deformation." *J Biomech Eng* 128 (2006): 925-33.

Okamoto, R. J., E. H. Clayton, and P. V. Bayly. "Viscoelastic Properties of Soft Gels: Comparison of Magnetic Resonance Elastography and Dynamic Shear Testing in the Shear Wave Regime." *Phys Med Biol* 56, no. 19 (Oct 7 2011): 6379-400.

Prange, M T, and S S Margulies. "Regional, Directional, and Age-Dependent Properties of the Brain Undergoing Large Deformation." *J Biomech Eng* 124 (2002): 244-52.

Prange, M T, D F Meaney, and S S Margulies. "Defining Brain Mechanical Properties: Effects of Region, Direction, and Species." *Stapp Car Crash J* 44 (2000): 205-13.

Prevost, T. P., G. Jin, M. A. de Moya, H. B. Alam, S. Suresh, and S. Socrate. "Dynamic Mechanical Response of Brain Tissue in Indentation in Vivo, in Situ and in Vitro." *Acta Biomater* 7, no. 12 (Dec 2011): 4090-101.

Qiu, G. Y., and T. J. Pence. "Remarks on the Behavior of Simple Directionally Reinforced Incompressible Nonlinearly Elastic Solids." *Journal of Elasticity* 49, no. 1 (1997): 1-30.

Romano, A., M. Scheel, S. Hirsch, J. Braun, and I. Sack. "In Vivo Waveguide Elastography of White Matter Tracts in the Human Brain." *Magn Reson Med* (Jan 17 2012).

Shuck, L Z, and S H Advani. "Rheological Response of Human Brain-Tissue in Shear." *Journal of Basic Engineering* 94 (1972): 905-11.

Smith, D. H., and D. F. Meaney. "Axonal Damage in Traumatic Brain Injury." *Neuroscientist* 6, no. 6 (2000): 483-95.

Spencer, Anthony J. M. *Continuum Theory of the Mechanics of Fibre-Reinforced Composites*. New York: Springer-Verlag, 1984.

Ueno, K., J. W. Melvin, L. Li, and J. W. Lighthall. "Development of Tissue Level Brain Injury Criteria by Finite Element Analysis." *J Neurotrauma* 12, no. 4 (Aug 1995): 695-706.

van Dommelen, J. A., T. P. van der Sande, M. Hrapko, and G. W. Peters. "Mechanical Properties of Brain Tissue by Indentation: Interregional Variation." *J Mech Behav Biomed Mater* 3, no. 2 (Feb 2010): 158-66.

Velardi, F., F. Fraternali, and M. Angelillo. "Anisotropic Constitutive Equations and Experimental Tensile Behavior of Brain Tissue." *Biomech Model Mechanobiol* 5, no. 1 (Mar 2006): 53-61.

Wright, R. M., and K. T. Ramesh. "An Axonal Strain Injury Criterion for Traumatic Brain Injury." *Biomech Model Mechanobiol* 11, no. 1-2 (Jan 2012): 245-60.

Zhang, L, K H Yang, and A I King. "A Proposed Injury Threshold for Mild Traumatic Brain Injury." *J Biomech Eng* 126 (2004): 226-36.